Development of acrylonitrile-butadiene-styrene composites with enhanced UV stability

R. M. Santos • G. L. Botelho • A. V. Machado

Abstract

Aiming to develop acrylonitrile-butadienestyrene (ABS) composites with enhanced ultraviolet stability, a series of formulations were prepared by melt compounding and evaluated by different characterization techniques. The influence of rutile titanium dioxide ($\mathrm{TiO_2}$) and its combination with furnace carbon black (CB) on the viscoelastic properties of neat ABS was studied by dynamic mechanical analysis. An increase in the glass transition (T_g) dynamics ascribed to the rubbery phase as a function of exposure time was observed. A greater contribution of CB nanoparticles in combination with $\mathrm{TiO_2}$ to minimize the modifications on the T_g of the butadienic component was clearly seen. Quasi-static and spectrophotometry results are in good agreement, showing the efficiency of $\mathrm{TiO_2}$ submicron particles and $\mathrm{CB/TiO_2}$ against photo-oxidative degradation of neat ABS. A different behaviour was observed for modified $\mathrm{ABS/TiO_2}$ and $\mathrm{ABS/\ CB/TiO_2}$ composites with light stabilizers, antioxidants and combinations of them. While the $\mathrm{TiO_2}$ efficiency was enhanced by the incorporation of combinations of light stabilizers and antioxidants, poor results were observed for modified $\mathrm{ABS/CB/TiO_2}$ composites as a consequence of antagonistic interactions. It was concluded that formulations of $\mathrm{ABS/CB/TiO_2}$ with light stabilizers and ultraviolet absorbers are unacceptable for common applications.

Introduction

Acrylonitrile-butadiene-styrene (ABS) is an impact-modified styrenic polymer used in most of their technological applications as a composite material reinforced with titanium dioxide ($\mathrm{TiO_2}$) and carbon black (CB) for remarkable property enhancements [1]. However, a common drawback of this material, bends and composites is its susceptibility to photo-oxidative degradation due to the slight activation energy of the hydrogen atom abstraction from the α carbon next to the 1,4 and 1,2 unsaturations of the rubbery phase [2,3].

Inorganic and organic pigments are primarily used to improve optical properties-appearance, shine and colour. In some cases, pigments also inhibit the photo-oxidative degradation of polymers by light scattering and filtering [4]. However, the ultraviolet (UV) durability of composites materials is dependent on the particle size, particle size distribution, surface properties, geometry shape, dispersion and interphase properties between the fillers and the polymeric matrix.

$\mathrm{TiO_2}$ or titania crystallizes in three main morphological structures: anatase (tetragonal, $\mathrm{D}_{4\,\mathrm{h}}^{19}-I4_1/mnm, a=b=3.782\text{Å}, c=9.502\text{Å}$), rutile (tetragonal, $\mathrm{D}_{4\,\mathrm{h}}^{14}-P4_2/$ mnm, $a=b=4.584\text{Å}, c=2.953\text{Å}$) and brookite (rhombohedrical, $\mathrm{D}_{2\,\mathrm{h}}^{15}-$ Pbca, $a=5.436\text{Å}, b=9.166\text{Å}$, $c=5.125\text{Å}$[5,6]. However, only the first two play an important role in industrial applications, because brookite $\mathrm{TiO_2}$ is rare and more difficult to prepare [7]. Rutile $\mathrm{TiO_2}$ is recognized to exhibit a greater stability, while anatase $\mathrm{TiO_2}$ is more photo-active acting as a catalytic of degradation [8]. The catalytic photo-activity of the $\mathrm{TiO_2}$ is explained by the transition of electrons from the valence to the conduction band. The excited electrons can react with oxygen leading to superoxy radical formation that is responsible for oxidizing the polymer. The positive holes formed in the valence band can reduce absorbed water to produce hydroxylic radicals which are also very reactive, interplaying a synergistic effect on degradation rate [9].

CB is a crystalline material with a complex structure, produced by several techniques: furnace, acetylene, channel, plasma and lampblack and, consequently, with different properties [10]. CB is widely used as spherical particles with a small diameter to improve the blackness and reduce the final cost of the composite. Although CB particles having large specific surface areas exhibit the best UV stabilities, difficulties associated with the dispersion during processing and poor interfacial interaction can limit its employment as reinforcement [11,12].

An overview of the literature reveals that there is a lack of work concerning the effect of $\mathrm{TiO_2}$ and CB to enhance ABS photo-stability. However, the exploitation of knowledge of ABS composites for tailored applications is an important issue for a successful selection of stabilized systems [13]. Thus, in this work, different compositions were prepared by melt compounding aiming to investigate the influence of $\mathrm{TiO_2}$ and $\mathrm{CB/TiO_2}$ combinations on the properties of neat ABS, especially on its performance against photo-oxidative degradation. Interactions of $\mathrm{ABS/\ TiO_2}$ and $\mathrm{ABS/CB/TiO_2}$ composites with light stabilizers, antioxidants and combinations of them will be also studied.

Experimental part

Raw material, fillers and stabilizers

ABS Terluran High Impact- 10® commercial available at the BASF (Ludwigshafen, Germany) is suitable for injection moulding and extrusion and was used as a raw material.

Rutile $\mathrm{TiO_2}$ Cristal 134$^{(R)}$ (from The National Titanium Dioxide Co. Ltd) is an alumina-/silica-modified rutile pigment obtained by chloride process (Table 1). $\mathrm{TiO_2}$ with a particle size of 220 nm was used taking into account that the ideal particle size for maximum light scattering should not be less than half the wavelength of the incident radiation ($400-700$ nm).

CB Printex 80® (from Degussa Japan Co., Ltd) was used as black filler without any purification step, and the most important properties are shown in Table 2.

A total of nine compositions containing light stabilizers, antioxidants and a combination of them were prepared for a successful selection of stabilized systems aiming to enhance ABS photo-stability. The stabilizers under studied are commercially available at the BASF.

Table 1 Typical properties of rutile $\mathrm{TiO_2}$ Cristal $134^{®}$

Properties	Values
$\mathrm{TiO_2}$ content	96.0-98.0 %
Aluminium hydroxide	1.0-3.0 %
Bulk density	$0.64 - 0.88\ \mathrm{kg/dm^3}$
Oil absorption	20.5 g/100 g pigment
pH	7.5

Table 2 Typical properties of carbon black Printex $80^{®}$

Properties	Values
Primary particle size	16 nm
DBP absorption	100 mL/100 g
Specific surface area	$220\ \mathrm{m^2/g}$
Tinting strength	124

Tinuvin $\mathrm{P}^{®}$ (2-(2'-hydroxy-5'-methylphenyl)benzotriazole); $M_{\mathrm{w}} = 225.4\ \mathrm{g/mol}$) and Chimassorb $119\mathrm{FL}^{®}$ (1,3,5-triazine-2,4,6-triamine, N,N'''-[1,2-ethanediylbis[[[4,6-bis-[butyl(1,2, 2,6,6-pentamethyl-4-piperidinyl) amino]-1,3,5-triazine-2-yl] imino]-3,1-propanediyl] bis[N',N''-dibutyl- N',N''-bis (1,2,2, 6,6-pentamethyl-4-piperidinyl); $M_{\mathrm{w}} = 2286\ \mathrm{g/mol}$) were used as ultraviolet absorbers (UVA) and hindered amine light stabilizers (HALS), respectively.

Irganox $1076^{®}$ (octadecyl-3-(3,5-di-tert.butyl-4-hydroxy-phenyl)-propionate); $M_{\mathrm{w}} = 531.0\ \mathrm{g/mol}$) and Irgafos $168^{(8)}$ (tris(2,4-di-ter-butylphenyl)phosphite); $M_{\mathrm{w}} = 646.9\ \mathrm{g/mol}$) were used as primary ($\mathrm{AO_1}$) and secondary ($\mathrm{AO_2}$) antioxidants, respectively.

Sample preparation

Dispersion of $\mathrm{TiO_2}$ and $\mathrm{CB/TiO_2}$

ABS composites containing $\mathrm{TiO_2}$ ($\mathrm{ABS/TiO_2}$) were obtained by compounding ABS Terluran HI- $10^{®}$ polymer, previously dried in an oven at 80°C during 1 h , with 3.0% (w/w) of $\mathrm{TiO_2}$ masterbatch, to produce white tapes. ABS samples containing combinations of CB with $\mathrm{TiO_2}$ (ABS/ $\mathrm{CB/TiO_2}$) were achieved by mixing the same amount of $\mathrm{TiO_2}$ masterbatch with 0.2%(w/w) of CB and a dispersing agent to avoid agglomeration and enhance its dispersion into polymeric matrix (ash tapes).

The TiO_2 masterbatch was obtained by dispersing the filler in a lower viscosity matrix, acrylonitrile-styrene (SAN) copolymer pellets, at high pressures in a Banbury industry internal mixer, originating a paste that was dried at room temperature and then triturated in a mill.

Samples preparation

ABS samples with different composition (Table 3) were prepared by melt compounding using a laboratory modular Leistritz LSM 30.34 intermeshing corotating twin-screw extruder, a temperature profile along the barrel from 170 to 220°C, a screw rotating of 100 rpm and a throughput of 4 kg/h. An extrusion die to produce tape (0.5 mm thickness) was used.

The extruded tapes (natural, white and ash) were cooled by water at constant temperature, of approximately 40°C, and dried with air. During sample processing, it was assured that the thickness remaining unchanged along the cross-section. This processing technique was used to produce tapes at low manufacturing cost and to simulate closely industrial production conditions.

Degradation procedure

Accelerated weathering experiments were carried out in a Xenotest 150*S* chamber from Heraeus (Original Hanau), in accordance with ISO 4892. During 2 h of ageing cycle, the specimens were exposed to 18.0 ± 0.5 min of rain period and the time remaining, 102.0 ± 0.5 min, was considered dry period.

In order to assure the reproductiveness of the results obtained in accelerated weathering studies, the xenon lamp

Table 3 ABS samples prepared by extrusion for weathering studies

Raw material	Additives					
ABS (phr)	TiO_2 (phr)	CB/TiO_2 (phr)	UVA (phr)	HALS (phr)	AO_1 (phr)	AO_2 (phr)
Unstabilized ABS samples						
100	-	-	-	-	-	-
100	3.0	-	-	-	-	-
100	3.0	0.2	-	-	-	-
ABS samples containing a combination of light stabilizers						
100	-	-	0.1	0.3	-	-

100	3.0	-	0.1	0.3	-	-
100	3.0	0.2	0.1	0.3	-	-
ABS samples containing a combination of antioxidants						
100	-	-	-	-	0.15	0.15
100	3.0	-	-	-	0.15	0.15
100	3.0	0.2	-	-	0.15	0.15
ABS samples containing a combination of light stabilizers and antioxidants						
100	-	-	0.1	0.3	0.15	0.15
100	3.0	-	0.1	0.3	0.15	0.15
100	3.0	0.2	0.1	0.3	0.15	0.15

phr parts per hundred

and their filters were replaced in agreement with the producer instructions.

Characterization techniques

Dynamical mechanical analysis (DMA) experiments were performed in a Seiko DMS 210 in a tension mode at 1 Hz . Measurements were performed from -110 to $150^{\circ}\mathrm{C}$ using a scanning rate of $2^{\circ}\mathrm{C/min}$, under a constant nitrogen flow. The viscoelastic properties of neat $\mathrm{ABS}, \mathrm{ABS/TiO_2}$ and $\mathrm{ABS/CB/TiO_2}$ composites were obtained as the average of three measurements.

The dispersion of $\mathrm{TiO_2}$ and $\mathrm{CB/TiO_2}$ in the polymeric matrix and the effects of UV radiation on the morphological properties of the ABS surface were evaluated by scanning electron microscopy (SEM) with a JEOL JSM6300 with an accelerating voltage of 20 kV and a magnification of 1000-20000×.

The total colour difference was measured with a Datacolor 650 TM spectrometer, using a D65 light source and 10° viewing angle. Colour changes (yellowing) during photo-oxidative degradation were obtained by CIE tristimulus values (L^*, a^* and b^*), according to CIELAB colour system.

The mechanical properties were evaluated in a Miniature Materials Tester (MINIMAT) from Polymer Laboratories, using a 200-N load cell. The stress versus strain curves were obtained with a deformation velocity $\mathrm{d}l/\mathrm{d}t = 0.2$ mm/min in the direction perpendicular to the machine orientation, at room temperature. For each composition and for each sample submitted to a specific degradation time, six specimens were tested and the sample thickness was measured with a pachymeter Mitutoyo with 0.025 mm of exactitude.

Results and discussion

Influence of TiO_2 and CB/TiO_2 on the properties of neat ABS

The influence of TiO_2 and CB/TiO_2 on the viscoelastic properties of neat ABS was evaluated by DMA, and the results are shown in Figs. 1 and 2.

ABS is an amorphous copolymer which exhibits two well-defined relaxation tan δ peak. The first centred at $-85^\circ C$ is related to the Brownian motion of the molecular chains at transition from the glassy to the rubbery state and is ascribed to the glass transition (T_g) dynamics of the amorphous chains of the butadiene (PB) [14]. This motion is slightly affected by the incorporation of TiO_2 and CB/ TiO_2 into ABS matrix due to the different interactions in

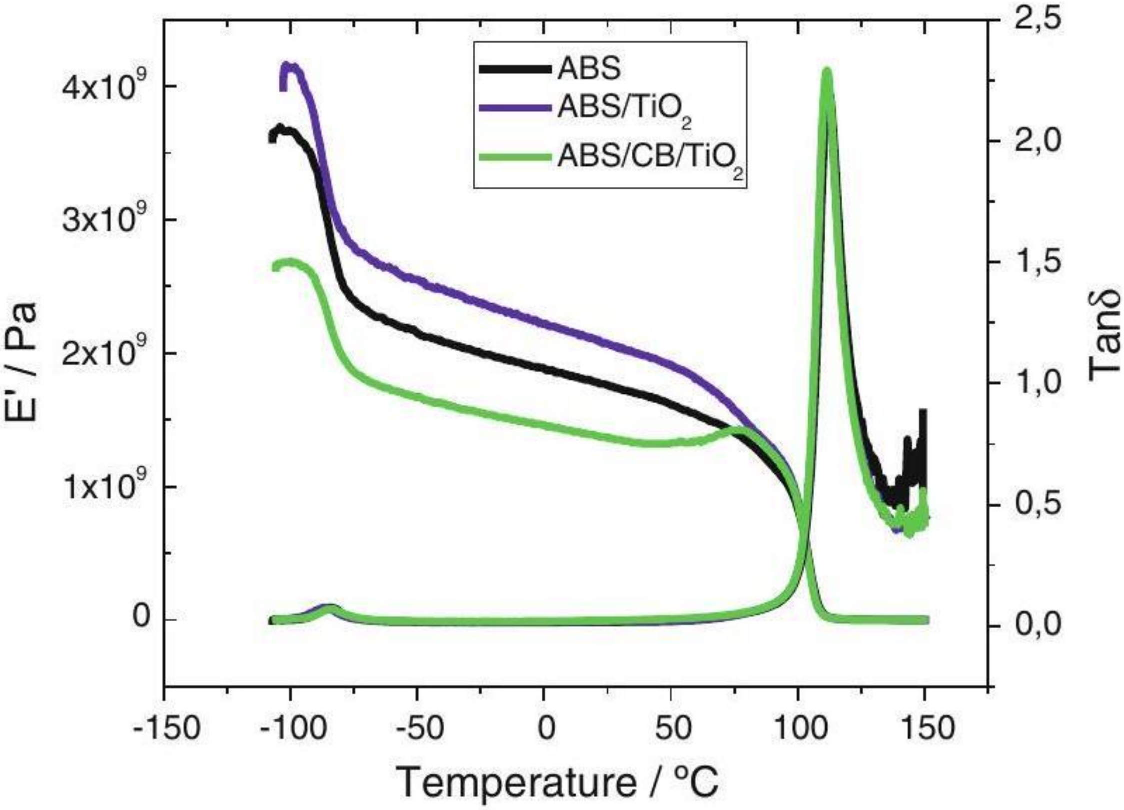

Fig. 1 Influence of TiO_2 and CB/TiO_2 on the damping (tan δ) and dynamic storage modulus (E') of neat ABS

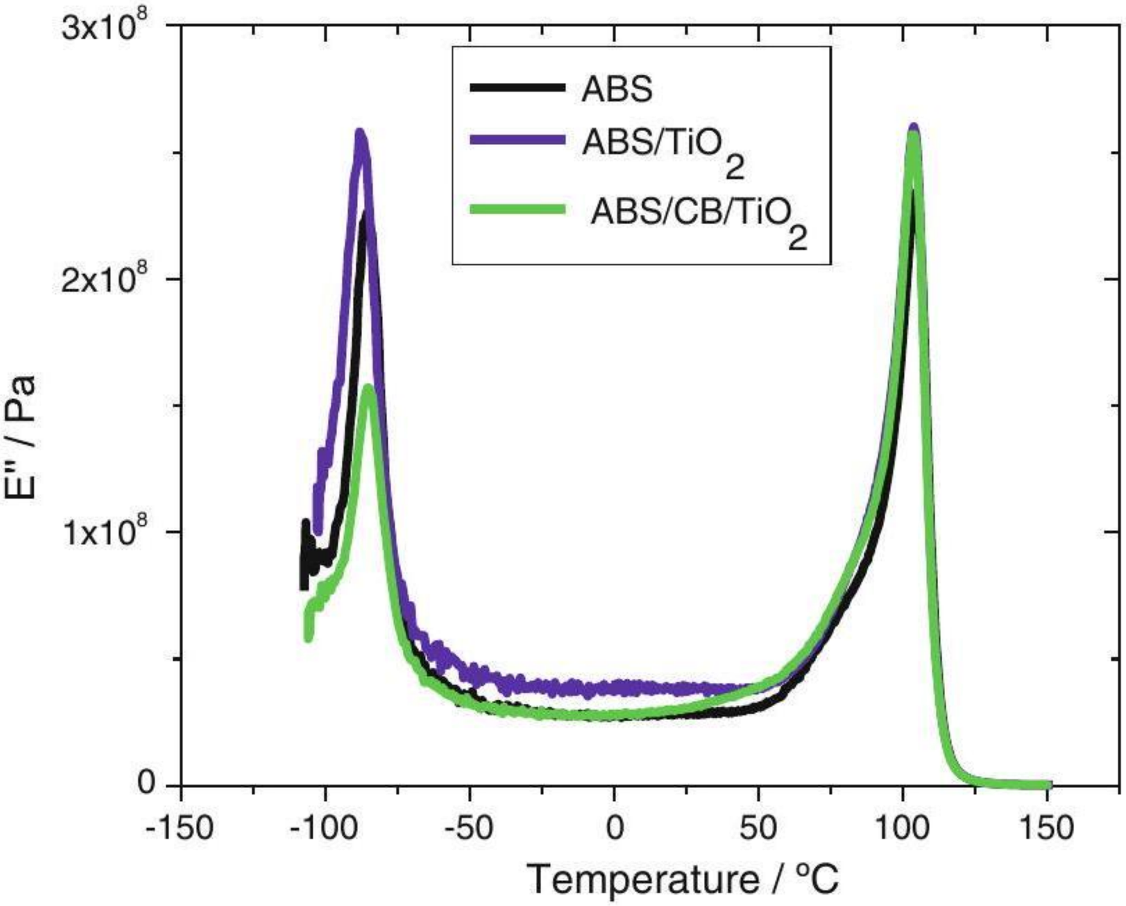

Fig. 2 Influence of $\mathrm{TiO_2}$ and $\mathrm{CB/TiO_2}$ on the loss modulus (E'') of neat ABS the interface layer surrounding the particles, as will be explained in more detail by the loss modulus results.

The second one appears near around $104^{\circ}\mathrm{C}$ corresponding to the relaxation process assigned to the T_g dynamics of acrylonitrile-styrene (SAN) phase, remaining unchanged by the addition of $\mathrm{TiO_2}$ and $\mathrm{CB/TiO_2}$ particles.

The effects of $\mathrm{TiO_2}$ and $\mathrm{CB/TiO_2}$ particles on the dynamic storage modulus (E') of neat ABS , an important property to assess the load-baring capacity of the polymeric matrix, are also given in Fig. 1. Even though all samples exhibit the same behaviour as a function of temperature, differences in E' values can be noted.

A prominent increase in the E' of the polymeric matrix with the incorporation of $\mathrm{TiO_2}$ was found, especially after the transition region of the rubbery phase, suggesting that the stiffness of ABS is enhanced due to the reinforcement effect imparted by $\mathrm{TiO_2}$ submicron particles. A poor behaviour was observed for ABS containing combinations of CB nanoparticles with $\mathrm{TiO_2}$, exhibiting the least value of the storage modulus. This result may be associated with the small dimension of CB nanoparticles (average particle size of 40 nm) and consequently with the poor dispersion degree achieved for $\mathrm{ABS/CB/TiO_2}$ composites. Cluster formation can occur, acting as a defect and inducing a decrease in the ABS stiffness [15]. This result can also suggest that a worst interaction between CB and TiO_2 particles with ABS matrix was accomplished, unable to provide a better degree of stress transfer at the interface.

The influence of TiO_2 and CB/TiO_2 on the loss modulus (E'') of neat ABS , a measure of the energy dissipated as heat per deformation cycle, is depicted in Fig. 2.

It can be observed a shift in the relaxation modes of the polymer molecules towards the lower temperatures ($T_g = -88°C$) for ABS samples containing TiO_2 with an average particle size of 220 nm . This behaviour can be explained by the repulsive interactions between the TiO_2 submicron particles and the polymer molecules, leading to an increase in the free volume and chain mobility with consequent decrease in the T_g [16].

ABS samples containing combinations of CB nanoparticles with TiO_2 show a lower loss modulus value but at the same temperature. While in neat ABS, the chains are fairly free to rotate, helping to minimize the overall energy of the sample, in samples containing CB/TiO_2, the movement of the polymer chains became some frozen, reducing the intensity of the cooperative motions of the amorphous chains, in good agreement with the results obtained by others [17].

The T_g dependence of ABS composites containing TiO_2 and CB/TiO_2 exposed to accelerated weathering conditions was determined by the onset of the loss modulus (E'') peak, and the results are depicted in Fig. 3.

A similar behaviour was found for neat ABS and ABS/TiO_2 composites, i.e. an increase in the T_g attributed to the PB phase as a function of exposure time due to oxidation of the rubbery phase by cross-linking with consequent reduction in the polymer chains mobility and free volume.

The contribution of CB nanoparticles in combination with TiO_2 to minimize the modifications on the T_g dynamics of the butadienic component is clearly seen and is probably associated with the multifunctional stabilizing effect of CB, acting as UV/Vis radiation absorber, H-donor and/or acceptor, quencher of excited state and hydroperoxide decomposer [11, 12].

Figure 4 shows the SEM micrographs of the surface of unexposed and exposed ABS/TiO_2 and $ABS/CB/TiO_2$ composites to 50 h of accelerated weathering conditions.

SEM micrographs of the surface of unexposed ABS/TiO_2 and $ABS/CB/TiO_2$ composites show that the TiO_2

Fig. 3T_g of the butadiene component (a) and acrylonitrile-styrene macrophase (b) of ABS, ABS/TiO_2 and $ABS/CB/TiO_2$ samples exposed to accelerated weathering conditions

butadiene
d
ene
f ABS, ABS/
B/TiO$_2$
to accelerated
tions

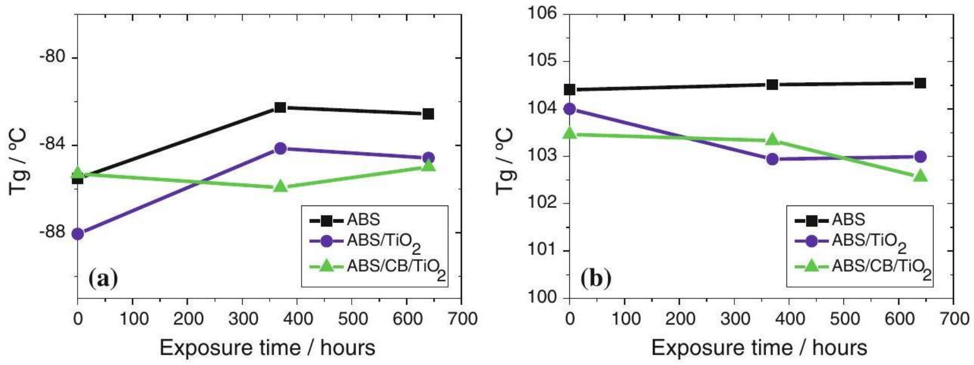

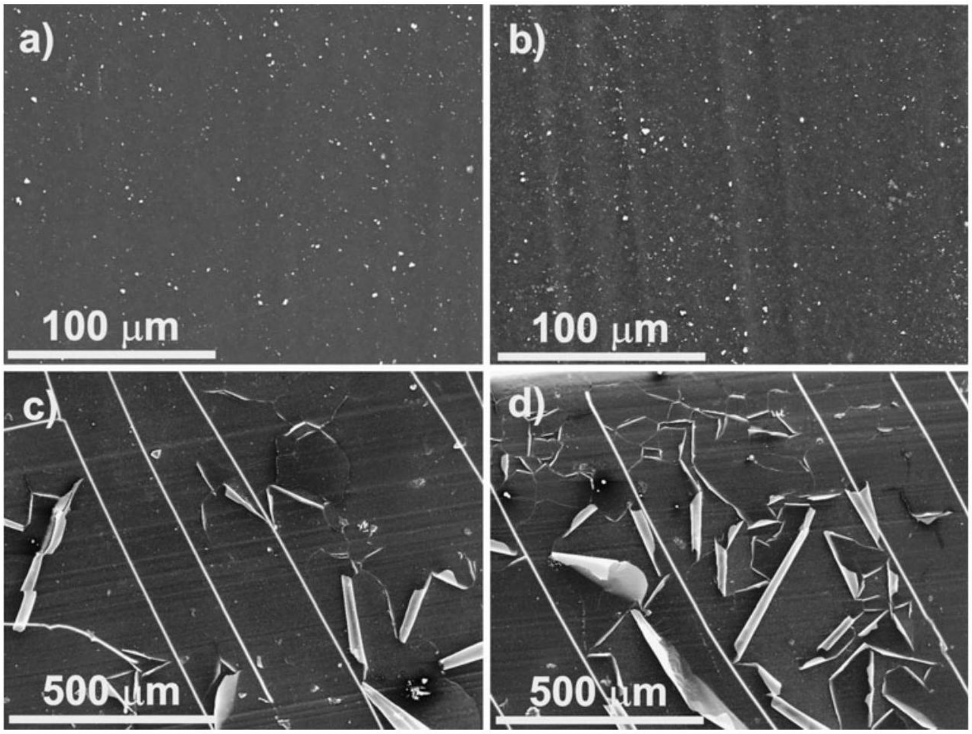

Fig. 4 SEM micrographs of the surface of unexposed (**a**, **b**) and exposed (**c**, **d**) ABS/TiO $_2$ and ABS/CB^2/TiO$_2$ composites to 50 h of accelerated weathering conditions microparticles are homogeneously distributed in the polymeric matrix. Slightly poor dispersion and some clusters can be observed for ABS samples containing combinations of CB nanoparticles with TiO$_2$ due to the electrostatic interactions and Van der Waals forces. Although the interphase thickness of composites containing CB is known to be around few nanometres [18], previous results obtained by DMA showed that the viscoelastic properties of ABS are affected even at the lower amounts of CB nanoparticles.

The exposure of ABS/TiO$_2$ and ABS/CB/TiO$_2$ composites to 50 h of accelerated weathering conditions induces drastic morphological changes, as it can be seen in Fig. 4c and d. Even though the degradation of ABS is a heterogeneous phenomenon which occurs preferentially at the irradiated surface, cracks formation and its propagation within the copolymer are observed and can compromised the mechanical performance of ABS, as will be shown in further stress-strain results.

Yellowing of ABS during processing and lifecycle is a serious problem from a technological point of view. According to Jouan and Gardette [19], the yellowing of ABS is due to degradation of the styrene in the macrophase SAN induced by radicals formed during the oxidation of PB. Thus, the formation of highly absorbing photo-products, such as α, β unsaturated ketones, is responsible for the ABS yellowing.

The influence of TiO_2 and CB/TiO_2 on the yellowness index (YI) of ABS samples submitted to different weathering conditions is shown in Fig. 5.

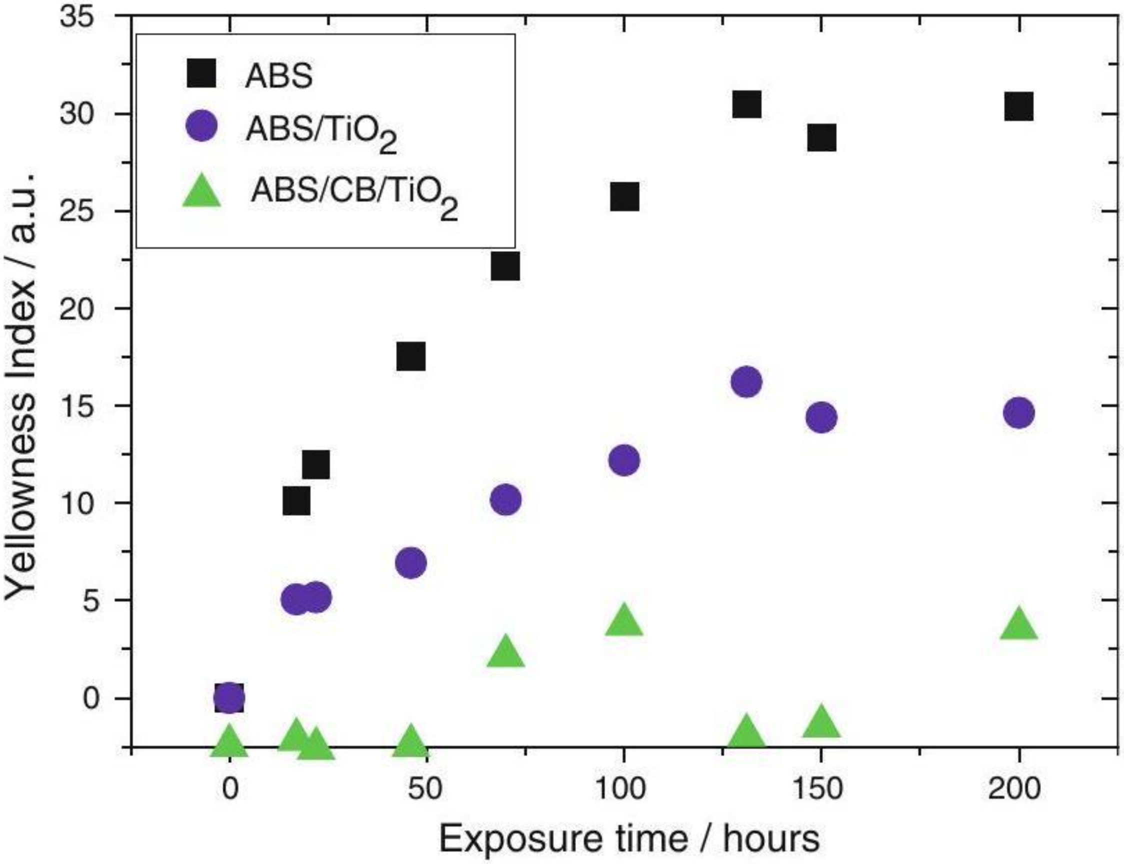

Fig. 5 Influence of TiO_2 and CB/TiO_2 on the YI of ABS samples submitted to accelerated weathering conditions

Although a similar trend was found for samples exposed to accelerated weathering experiments, i.e. an increase in yellowing rate as a function of the exposure time, TiO_2 and CB/TiO_2 have a positive effect on ABS YI . The results show the efficiency of the TiO_2 and CB/TiO_2 against colour modifications, by absorbing and/or screening UV radiation through different stabilization mechanism [4, 11, 20].

Since in literature it is well known that the incorporation of fillers into polymeric matrix affects its intrinsic mechanical properties, the influence of TiO_2 and CB/TiO_2 particles on the elongation at break [$\varepsilon_b(t0)$] of neat ABS was studied and the results are shown in Table 4.

It was found that elongation at break of neat ABS is enhanced by the incorporation of $\mathrm{TiO_2}$, corroborated by SEM results and suggesting that a good interaction between the submicron particles and polymeric matrix was achieved. A different behaviour can be observed for ABS/ $\mathrm{CB/TiO_2}$ composites which exhibit the lowest initial value of $\varepsilon_{\mathrm{b}(t0)}$ due probably to the worst CB nanoparticles dispersion in the polymer matrix.

There are a series of studies that discuss the mechanical behaviour of polymer systems containing fillers [21-26]. However, up to our knowledge, there is a lack of reports regarding the effects of $\mathrm{TiO_2}$ and $\mathrm{CB/TiO_2}$ interactions on the mechanical and especially on the UV mechanical performance of ABS [15, 27].

Table 4 Influence of $\mathrm{TiO_2}$ and $\mathrm{CB/TiO_2}$ on the elongation at break of neat ABS

Samples code	Elongation at break (%)
ABS	128 ± 16
$\mathrm{ABS/TiO_2}$	162 ± 24
$\mathrm{ABS/CB/TiO_2}$	99 ± 8

The effects of $\mathrm{TiO_2}$ and $\mathrm{CB/TiO_2}$ on the UV mechanical performance of ABS are presented in Fig. 6.

The inclusion of $\mathrm{TiO_2}$ and $\mathrm{CB/TiO_2}$ into polymeric matrix leads to an increase in the ABS mechanical performance exposed to accelerated weathering conditions. The decrease in elongation at break of samples as a function of exposure time is associated with the oxidation of the rubbery phase by cross-linking (Fig. 3) and also with the cracks formation at the surface (Fig. 4c, d).

Influence of $\mathrm{TiO_2}$ and $\mathrm{CB/TiO_2}$ on the properties of modified ABS composites with different stabilized systems

The influence of $\mathrm{TiO_2}$ and $\mathrm{CB/TiO_2}$ particles on the optical and mechanical properties of modified ABS composites with light stabilizers (Chimassorb 119FL® and Tinuvin P®), antioxidants (Irganox 1076 ® and Irgafos 168®) and combinations of them was also investigated.

Figure 7 shows the YI of modified $\mathrm{ABS/TiO_2}$ and ABS/ $\mathrm{CB/TiO_2}$ composites exposed to accelerated weathering conditions, respectively.

It can be observed an enhancement of the $\mathrm{TiO_2}$ efficiency in protecting ABS against colour modifications with incorporation of stabilizers into polymer matrix. Although a very similar behaviour was observed for modified ABS/ $\mathrm{TiO_2}$ composites with light stabilizers ($\mathrm{ABS/TiO_2/HALS/}$ UVA) and with antioxidants ($\mathrm{ABS/TiO_2/AO}$), advantages were found when combinations of light stabilizers were used with phenolic and trivalent organophosphorus antioxidants, suggesting that a synergistic effect was achieved. This behaviour can be the result of the light stabilizers and

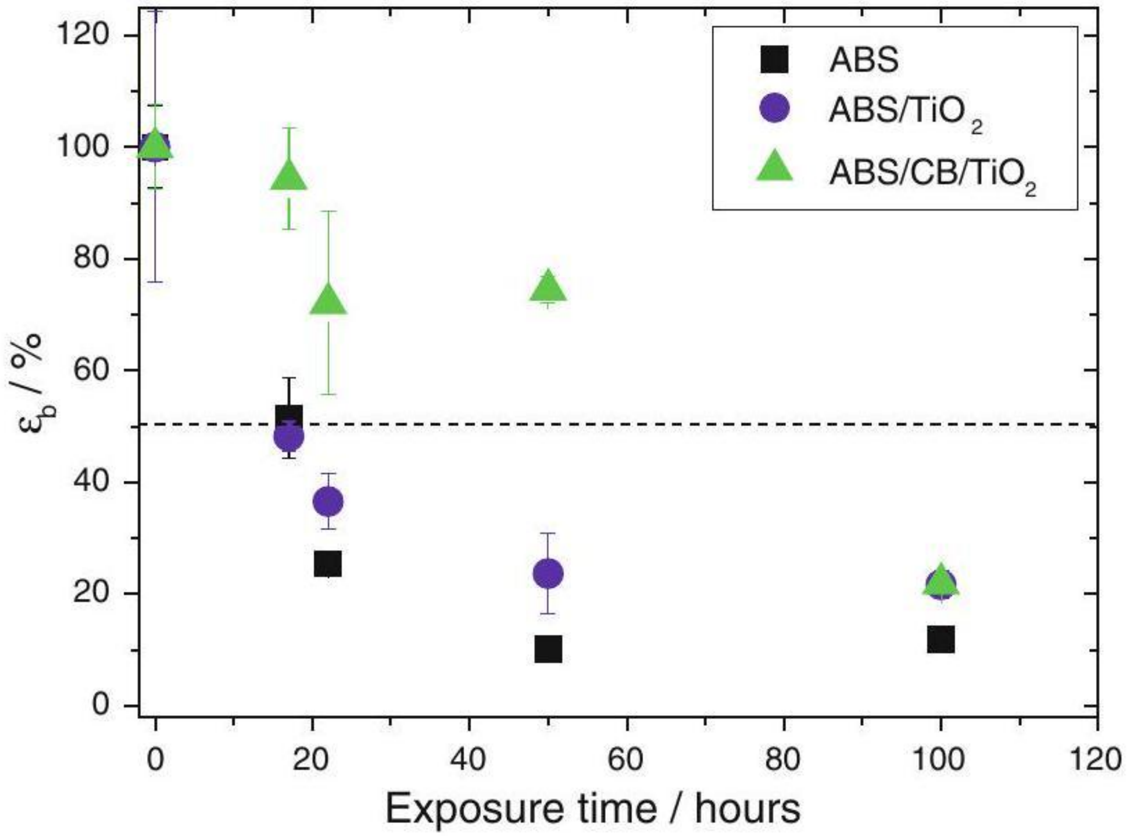

Fig. 6 The effects of TiO_2 and CB/TiO_2 on the UV mechanical performance of ABS

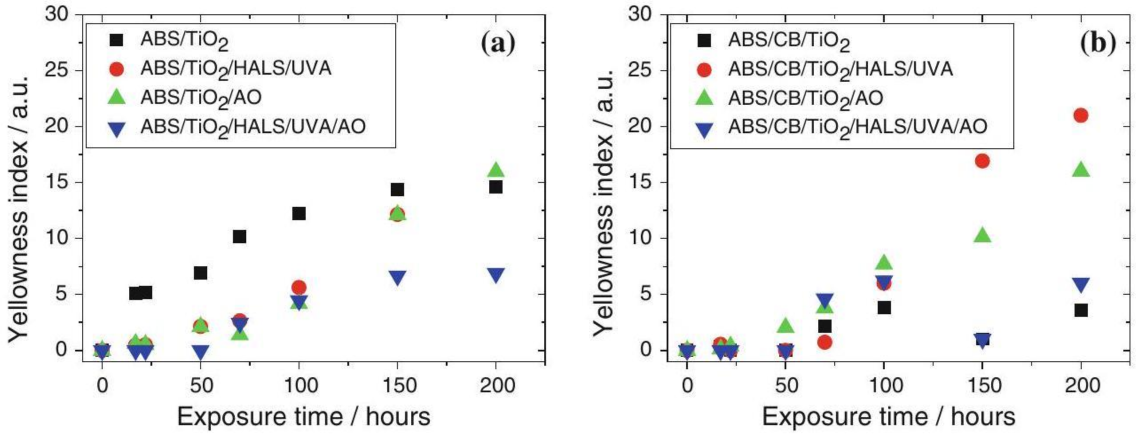

Fig. 7 Yellowness index of modified **a**ABS/TiO_2 and **b**$ABS/CB/TiO_2$ composites exposed to accelerated weathering conditions, respectively

Fig. 8 Influence of TiO_2 and CB/TiO_2 on the mechanical properties of modified ABS composites with different stabilized systems exposed to accelerated weathering conditions, respectively

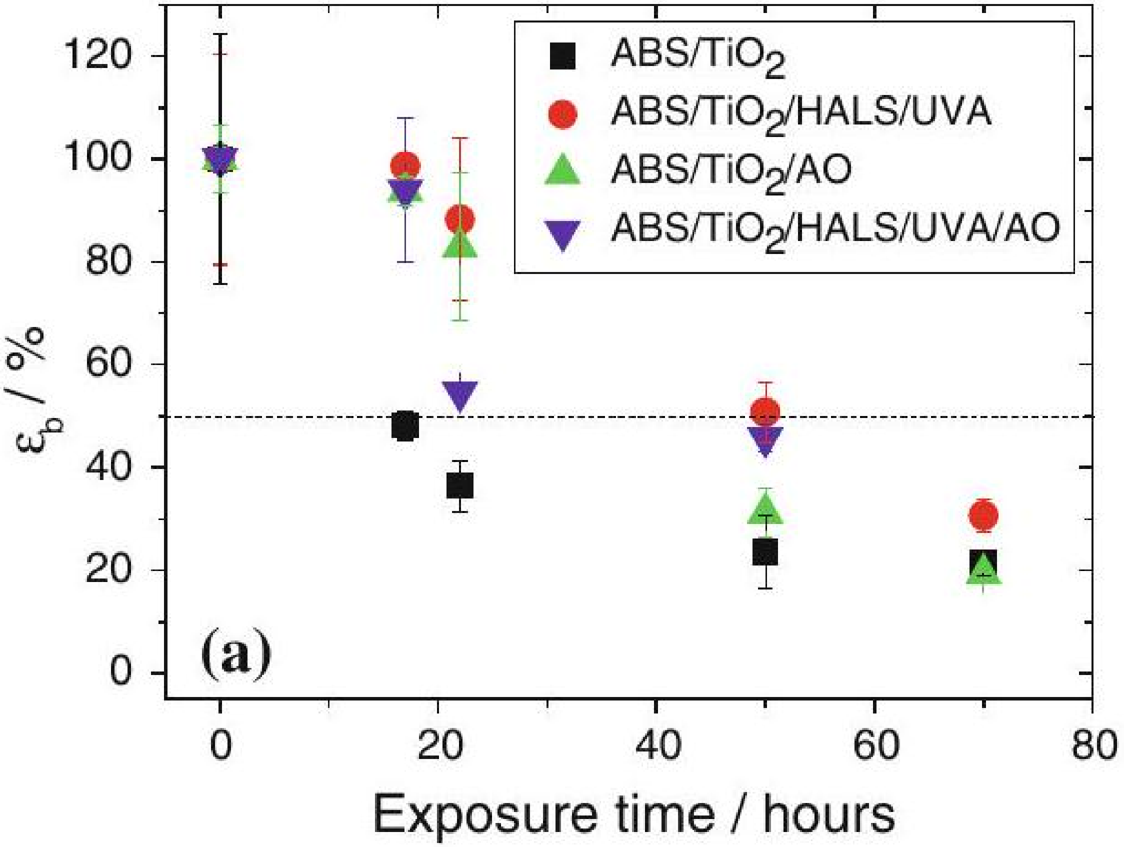ABS/TiO$_2$
ABS/TiO$_2$/HALS/UVA
ABS/TiO$_2$/AO
ABS/TiO$_2$/HALS/UVA/AO
ε_b / %
Exposure time / hours
0
20
40
60
80
100
120
0
20
40
60
80
(a)

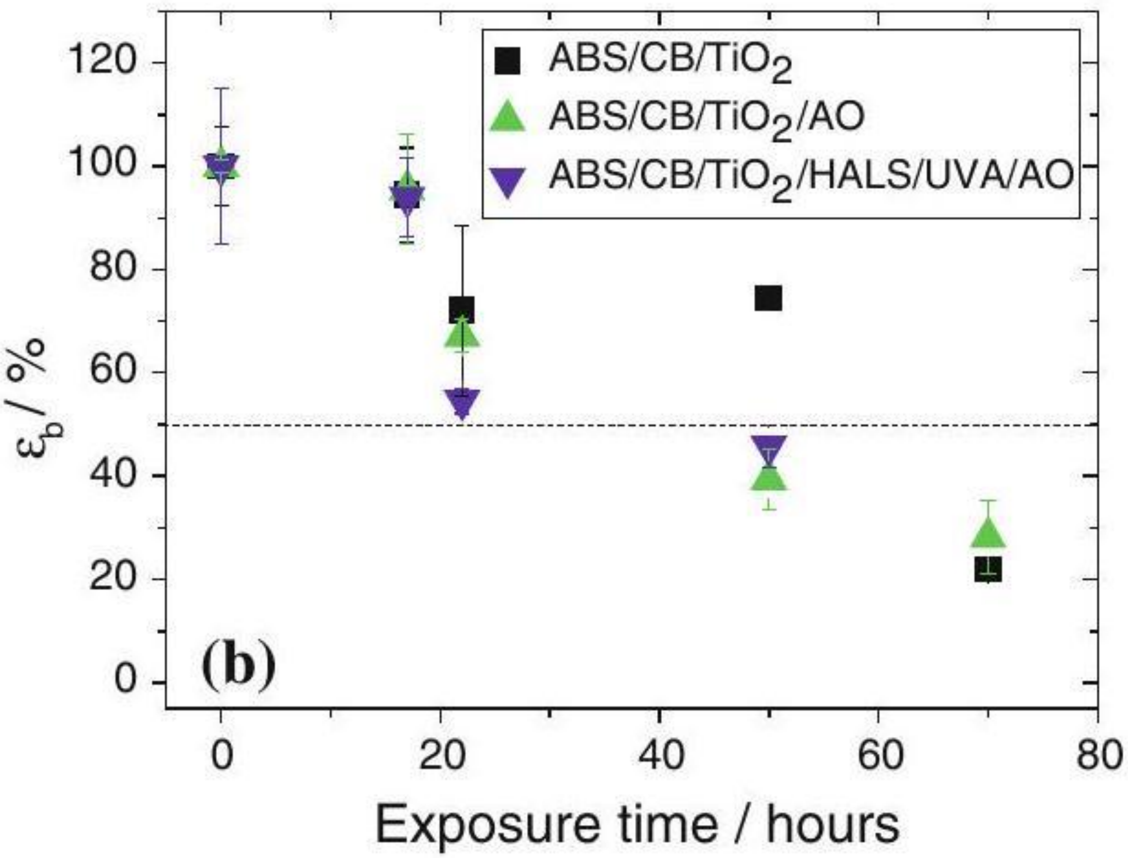

antioxidants playing a complementary role, inducing a restraint of the α, β unsaturated ketones formed during photo-oxidative degradation process.

An interesting feature of the data from Fig. 7 b is the existence of antagonistic effects in modified $\mathrm{ABS/CB/TiO_2}$ composites with light stabilizers and with antioxidants.

However, poor results were found for filled samples containing a combination of Tinuvin P$^{(8)}$ and Chimassorb 119 FL ®. This behaviour is associated with the activity of the surface groups on CB, such as carboxyl, quinines, phenols, carboxylphenols, lactones, aldehydes, ketones, anhydrides and others, resulting in antagonistic interactions [8]. The formation of hydrogen bonds between the CB oxygen-containing groups and the amine resulting in sterically hindered proton transfer reactions with consequent decrease in the activity and stabilizing effect of the HALS [28].

The influence of $\mathrm{TiO_2}$ and $\mathrm{CB/TiO_2}$ on the mechanical properties of modified ABS composites with different stabilized systems exposed to accelerated weathering conditions is shown in Fig. 8.

According to the obtained data, combinations of light stabilizers with antioxidants enhance the efficiency of rutile $\mathrm{TiO_2}$ against the photo-oxidative degradation of ABS under accelerated weathering conditions. For composites containing combinations of CB nanoparticles with $\mathrm{TiO_2}$, it was observed that the mechanical performance decreases with

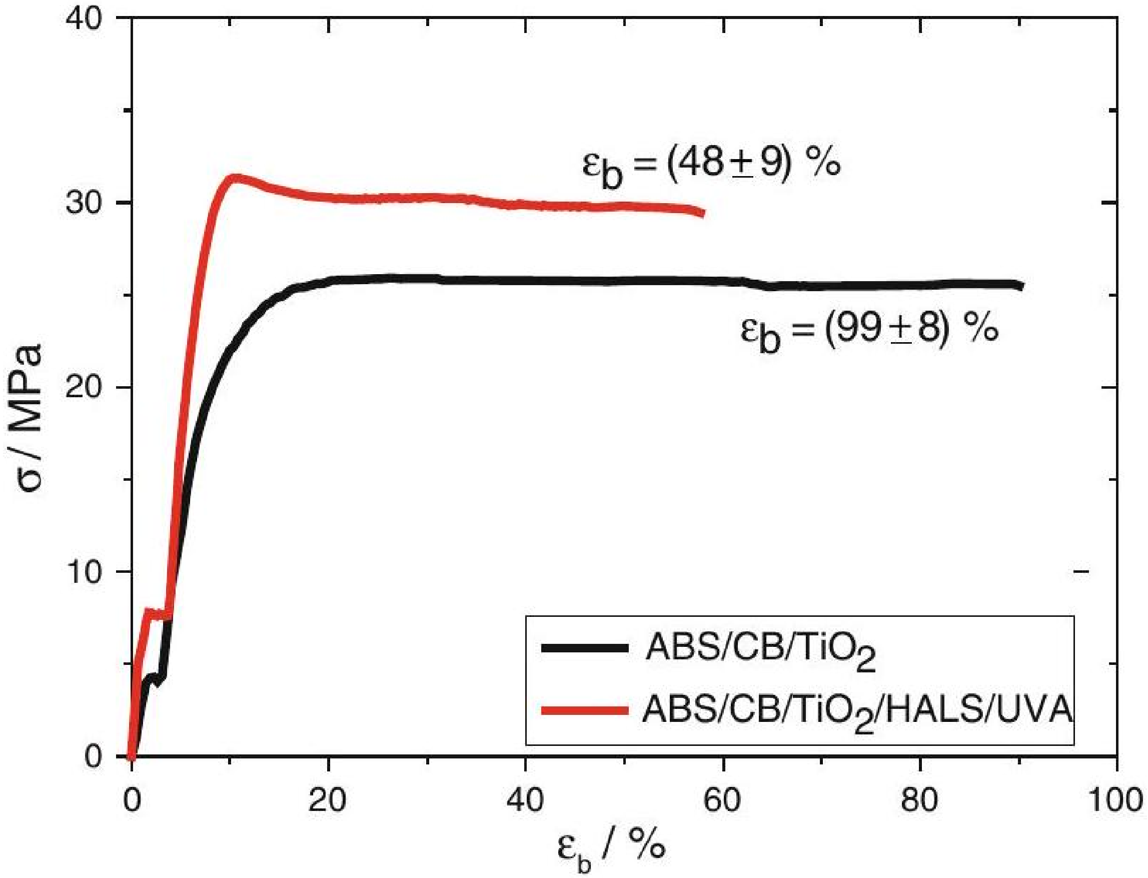

Fig. 9 Stress-strain curves of unexposed ABS/CB/TiO_2 and combinations of ABS/CB/TiO_2 with HALS and UVA

the incorporation of light stabilizers and antioxidants as a consequence of antagonistic interactions. However, poor results were achieved for ABS/CB/TiO_2 composites containing combinations of UVA and hindered amines light stabilizers, as it can be seen in Fig. 9.

Figure 9 shows that the elongation at break of unexposed ABS/CB/TiO_2 composites with Chimassorb 119FL® and Tinuvin P® ($48 \pm 9\%$) is significantly lower than the ABS/CB/TiO_2 composites ($99 \pm 8\%$), corroborating with findings obtained previously. As explained above, this behaviour can be associated with the adsorption of hindered amines light stabilizers onto surface of CB resulting in antagonistic interactions [29], becoming this specific formulation unacceptable for common applications.

Antagonistic effects were also observed in samples containing combinations of Irgafos 168® and Irganox 1076 $^{(B)}$, although these are less pronounced. This behaviour can be explained taking into account that the phosphite group, characteristic of Irgafos 168®, is located in the core of the molecule and can be obstructed by alkyl groups being highly hindered from interaction. On the other hand, the chemical structure of Irganox 1076 $^{(8)}$ results in a moderate adsorption activity due to the higher steric accessibility of the ester group [30]. According to Peña et al. [30], the shape of the molecule also plays an important role on the adsorption activity. Generally, rodshaped molecules show higher adsorption activity (as Irganox 1076 $^{(8)}$) in comparison with square-shaped molecular structures.

Conclusions

A series of ABS composites were prepared by melt compounding and submitted to accelerated weathering conditions with the aim at developing $\mathrm{ABS/TiO_2}$ and $\mathrm{ABS/CB/\ TiO_2}$ composites with enhanced UV stability.

The results obtained by DMA showed the contribution of $\mathrm{CB/TiO_2}$ particles to minimize the modifications on the T_g dynamics of the PB , which is associated with its stabilization mechanism.

Yellowing measurements showed that rutile $\mathrm{TiO_2}$ and $\mathrm{CB/TiO_2}$ combination have a significant influence on photo-chemical stability of the ABS, exhibiting a protective effect against colour modifications.

Mechanical properties of ABS samples are significantly affected during accelerated weathering conditions mainly due to the cross-linking of the butadienic component and crack formation at the irradiated surface. However, it was found that the mechanical performance of ABS exposed to weathering conditions is less affected with the incorporation of $\mathrm{TiO_2}$ and $\mathrm{CB/TiO_2}$ particles.

A different behaviour was found for modified $\mathrm{ABS/TiO_2}$ and $\mathrm{ABS/CB/TiO_2}$ composites with light stabilizers, antioxidants and combinations of them. Although the $\mathrm{TiO_2}$ efficiency in protecting ABS against photo-oxidative degradation is enhanced when light stabilizers and antioxidants were used, best results were achieved with combinations of them, suggesting that synergistic effects were found. Contrarily, modified $\mathrm{ABS/CB/TiO_2}$ composites showed that antagonistic effects were observed, although poor results were achieved for combinations with Chimassorb 119FL® and

Tinuvin $\mathrm{P^{(R)}}$, becoming this formulation unacceptable for common applications.

Acknowledgements The authors would like to thank the Portuguese Foundation for the Science and Technology (FCT) and PoliversalPlásticos e Tecnologia, S.A. for the PhD grant SFRH/BDE/15657/ 2007.

References

1. Adams E, DJBMEA, Colborn RE, Buckley DJ, Colborn RE (1993) Acrylonitrile butadiene styrene polymers. Rapra Technology, Shawbury
2. Santos RM, Pimenta A, Botelho G, Machado AV (2013) Polym Test 32:78. doi:10.1016/j.polymertesting.2012.08.013
3. Santos RM, Botelho GL, Machado AV (2010) J Appl Polym Sci 116:2005. doi:10.1002/app. 31663
4. Allen NS, Edge M, Corrales T et al (1998) Polym Degrad Stab 61:183. doi:10.1016/S0141-3910(97)00114-6
5. Winkler J (2003) Titanium dioxide. Vincentz Network, Hannover
6. Diebold U (2003) Surf Sci Rep 48:53. doi:10.1016/S0167-5729(02)00100-0
7. Landmann M, Rauls E, Schmidt WG (2012) J Phys 24: 195503

8. Allen NS, Edge M, Ortega A et al (2004) Polym Degrad Stab 85:927. doi:10.1016/j.polymdegradstab.2003.09.024
9. Farrokhpay S (2009) Adv Colloid Interface Sci 151:24. doi:10. 1016/j.cis.2009.07.004
10. Donnet JB, Bansal RC, Wang MJ (1993) Carbon black: science and technology. Taylor & Francis, London
11. Horrocks AR, Mwila J, Miraftab M, Liu M, Chohan SS (1999) Polym Degrad Stab 65:25. doi:10.1016/S0141-3910(98)00213-4
12. Liu M, Horrocks AR (2002) Polym Degrad Stab 75:485. doi:10. 1016/S0141-3910(01)00252-X
13. Iannuzzi G, Mattsson B, Rigdahl M (2012) Polym Eng Sci. doi:10.1002/pen. 23438
14. Kotsilkova R, Fragiadakis D, Pissis P (2005) J Polym Sci 43:522. doi:10.1002/polb. 20352
15. Shenavar A, Abbasi F (2007) J Appl Polym Sci 105:2236. doi:10. 1002/app. 26219
16. Hamming LM, Qiao R, Messersmith PB, Catherine Brinson L (2009) Compos Sci Technol 69:1880. doi:10.1016/j.compscitech. 2009.04.005
17. Fragneaud B, Masenelli-Varlot K, Gonzalez-Montiel A, Terrones M, Cavaillé JY (2008) Compos Sci Technol 68:3265. doi:10. 1016/j.compscitech.2008.08.013
18. Ma P-C, Siddiqui NA, Marom G, Kim J-K (2010) Composites A 41:1345. doi:10.1016/j.compositesa.2010.07.003
19. Jouan X, Gardette JL (1992) Polym Degrad Stab 36:91. doi:10. 1016/0141-3910(92)90054-9
20. Allen NS, Khatami H, Thompson F (1992) Eur Polym J 28:817. doi:10.1016/0014-3057(92)90089-K
21. Wu S (1985) Polymer 26:1855. doi:10.1016/0032-3861(85) 90015-1
22. Wu S (1990) Polym Eng Sci 30:753. doi:10.1002/pen. 760301302
23. Selvin TP, Kuruvilla J, Sabu T (2004) Mater Lett 58:281. doi:10. 1016/S0167-577X(03)00470-1
24. Thomas PC, Tomlal Jose E, Selvin Thomas P, Thomas S, Joseph K (2010) Polym Compos 31:1515. doi:10.1002/pc. 20938
25. Thomas SP, Thomas S, Bandyopadhyay S (2009) Composites A 40:36. doi:10.1016/j.compositesa.2008.10.005
26. Ghosh P, Chakrabarti A (2000) Eur Polym J 36:1043. doi:10. 1016/S0014-3057(99)00157-3
27. Duan Y, Liu S, Wang G, Guan H, Wen B (2006) J Appl Polym Sci 102:1839. doi:10.1002/app. 24014
28. Peña JM, Allen NS, Edge M, Liauw CM, Valange B (2001) Polym Degrad Stab 72:259. doi:10.1016/S0141-3910(01)00033-7
29. Haacke G, Longordo E, Brinen JS, Andrawes FF, Campbell BH (1999) J Coat Technol 71:87. doi:10.1007/bf02697890

30. Peña JM, Allen NS, Edge M et al (2001) J Mater Sci 36:2885. doi:10.1023/a:1017998202931